Key Points:
- A global validation of MODIS and AMSR-E SSTs is completed
- AMSR-E v7 has biasing at low values of water vapor; a correction is suggested
- MODIS c5 has cloud contamination in night SST retrievals at surface temperatures $<10°C$

Correspondence to:
C. L. Gentemann,
gentemann@remss.com

Three way validation of MODIS and AMSR-E sea surface temperatures

Chelle L. Gentemann[1]

[1]Remote Sensing Systems, Santa Rosa, California, USA

Abstract The estimation of retrieval uncertainty and stability are essential for the accurate interpretation of data in scientific research, use in analyses, or numerical models. The primary uncertainty sources of satellite SST retrievals are due to errors in spacecraft navigation, sensor calibration, sensor noise, retrieval algorithms, and incomplete identification of corrupted retrievals. In this study, comparisons to in situ data are utilized to investigate retrieval accuracies of microwave (MW) SSTs from the Advanced Microwave Scanning Radiometer—Earth Observing System (AMSR-E) and infrared (IR) SSTs from the Moderate Resolution Imaging Spectroradiometer (MODIS). The highest quality MODIS data were averaged to 25 km for comparison. The in situ SSTs are used to determine dependencies on environmental parameters, evaluate the identification of erroneous retrievals, and examine biases and standard deviations (STD) for each of the satellite SST data sets. Errors were identified in both the MW and IR SST data sets: (1) at low atmospheric water vapor a posthoc correction added to AMSR-E was incorrectly applied and (2) there is significant cloud contamination of nighttime MODIS retrievals at SST $<10°C$. A correction is suggested for AMSR-E SSTs that will remove the vapor dependency. For MODIS, once the cloud contaminated data were excluded, errors were reduced but not eliminated. Biases were found to be $-0.05°C$ and $-0.13°C$ and standard deviations to be $0.48°C$ and $0.58°C$ for AMSR-E and MODIS, respectively. Using a three-way error analysis, individual standard deviations were determined to be $0.20°C$ (in situ), $0.28°C$ (AMSR-E), and $0.38°C$ (MODIS).

1. Introduction

Sea surface temperature (SST) is a key climate and weather measurement routinely used in numerical weather prediction (NWP), atmospheric, oceanographic, fisheries, climate, and other sciences. While the long-term record of SST begins with bucket temperatures taken from sailing ships, modern SST measurements are made by moored buoy, drifting buoy, ship intake, ship CTD casts, in situ radiometers carried on research vessels, and satellites. Many of these in situ measurements are reported in near-real-time (NRT) on the global telecommunication system (GTS) for use in ocean prediction, weather forecasting, and fisheries prediction. While easily available, they are only single point measurements made in a very large ocean. Better spatial coverage is provided by satellite observations of SST, from both microwave (MW) and infrared (IR) radiometers carried on a number of satellites. The MW instruments are able to measure SST in all weather conditions except rain, providing exceptional coverage, but at a spatial resolution of $\sim$50 km. IR instruments are able to measure SST at a spatial resolution of 1 km, but are unable to measure through cloud cover and therefore have limited availability in cloudy regions.

Validation of satellite SST retrievals is complicated by several important differences between satellite and in situ SST measurements. First, it needs to be recognized that there is significant spatial/temporal inhomogeneity between in situ and satellite measurements. In situ measurements are usually 90 s (drifters) to 60 min (moored) time averages of SSTs at a single point, while satellite measurements are instantaneous measurements averaged over a large spatial footprint [*Lumpkin and Pazos*, 2007; Pacific Marine Environmental Laboratory (PMEL), TAO/TRITON Data Sampling Regimes, 2013, http://www.pmel.noaa.gov/tao/proj_over/sampling.html]. In coastal regions where spatial variability of SST is high, satellite buoy comparisons have a higher standard deviation (STD) due to the difference in spatial sampling between the satellites and buoy measurements [*Castro et al.*, 2012]. A portion of the derived uncertainty can be attributed to this spatial mismatch and is a geophysical difference rather than an instrument or processing error.

Next the SST measurements are taken at different depths: IR SST is a skin SST measurement penetrating only a few microns, MW SST is a subskin measurement penetrating to a few millimeters, and moored and

drifting buoys typically measure at 0.2–1.5 m depth. At the ocean surface, there is a heat flux into the atmosphere which creates a cool skin of ocean water at the surface. This layer is generally 0.5–0.17°C cooler then the subskin waters [*Donlon et al.*, 2002; *Jessup and Branch*, 2008; *Minnett et al.*, 2011]. To compare the subsurface MW and 1 m in situ data to the IR retrievals, the IR retrievals need to have the cool skin effect accounted for. Additionally, while the upper ocean is usually well mixed and the 1 mm and 1 m measurements can be directly compared, a decoupling of the surface and 1 m SSTs can occur during the daytime at low winds due to solar heating [*Price et al.*, 1986; *Soloviev and Lukas*, 1997; *Ward*, 2006; *Webster et al.*, 1996]. We will examine the data for this effect and attempt to minimize its impact on our results.

2. Data Sets

The AQUA satellite carries both MW and IR instruments capable of retrieving SST: the Advanced Microwave Scanning Radiometer—Earth Observing System (AMSR-E) and the Moderate Resolution Imaging Spectrora-diometer (MODIS). AQUA was launched on 4 May 2002 with SST retrievals first available on 1 June 2002 (AMSR-E) and 4 July 2002 (MODIS). AMSR-E was put into safe-mode on 4 October 2011 and data are not available since that date. MODIS continues to provide data at present. While both MODIS and AMSR-E SSTs are widely used for research and operations and each have been previously validated in some manner, there has been no detailed analysis of environmental variable dependencies and temporal stability. This study pairs these virtually simultaneous satellite SST retrievals with in situ SST measurements made by drifting and moored buoys. These collocated measurements are used to examine global errors, stability of the retrievals, and to investigate sources of errors. The three independent SST measurements allow for a three-way error analysis which can designate individual measurement errors.

The MODIS and AMSR-E SST data sets are ideal for this triple collocation analysis because both operate on the AQUA satellite, so the SST retrievals are virtually simultaneous. MODIS scans directly downward while AMSR-E scans forward at a 55° angle, leading to an ∼1 min difference in observation of the same surface area. The exact difference depends on the AMSR-E scan angle. The MODIS and AMSR-E SST retrieval methodologies are independent and the errors inherent in IR and MW SST retrieval are fundamentally different. Both instruments can have instrumental errors or calibration issues that impact SST retrievals. SST retrieval errors in AMSR-E are likely from a number of sources: errors in the geophysical retrieval algorithm, errors in the inputs to the geophysical retrieval algorithm (wind direction), radio frequency interference (RFI), undetected rain and/or undetected sea ice [*Gentemann et al.*, 2010b]. Errors in the MODIS SST are likely from atmospheric absorption and undetected cloud or fog [*Brown and Minnett*, 1999].

2.1. AMSR-E

National Aeronautics and Space Administration's (NASA) Aqua satellite, launched 4 May 2002, carries the Japan Aerospace eXploration Agency (JAXA)'s AMSR-E instrument. AMSR-E has 10 channels corresponding to five frequencies (7, 11, 19, 24, and 37 GHz) and two polarizations (vertical and horizontal). While the Tropical Rainfall Measuring Mission (TRMM) Microwave Imager (TMI) has been providing accurate SSTs within 40° of the equator [*Wentz et al.*, 2000], AMSR-E is the first polar orbiting microwave radiometer capable of accurately measuring global SSTs since the poorly calibrated Scanning Multichannel Microwave Radiometer (SMMR) was launched in 1987 [*Wentz et al.*, 2000]. AMSR-E orbits at an altitude of 705 km, with a 1.6 m antenna, resulting in a ground swath width of 1450 km.

Between 4 and 11 GHz, the vertically polarized brightness temperature (T_B) of the sea-surface has an appreciable sensitivity to SST. In addition to SST, T_B depends on the sea-surface roughness and the atmospheric temperature and moisture profiles. Fortunately, AMSR-E measures multiple frequencies that are more than sufficient to remove the surface-roughness and atmospheric effects. Sea-surface roughness, which is tightly correlated with the local wind, is usually parameterized in terms of the near-surface wind speed and direction. The 7 GHz channel present on AMSR-E, provides improved estimates of sea-surface roughness and improved accuracy for SSTs less than 12°C [*Gentemann et al.*, 2010a]. All channels are used to simultaneously retrieve SST, wind speed, columnar water vapor, cloud liquid water, and rain rate [*Wentz and Meissner*, 2000]. These environmental variables are calculated using a multistage linear regression algorithm derived through comprehensive radiative transfer model simulations.

SST retrieval is prevented only in regions with sun-glitter, rain, near land, and radio frequency interference (RFI). Since only a small number of retrievals are unsuccessful, almost complete global coverage is achieved
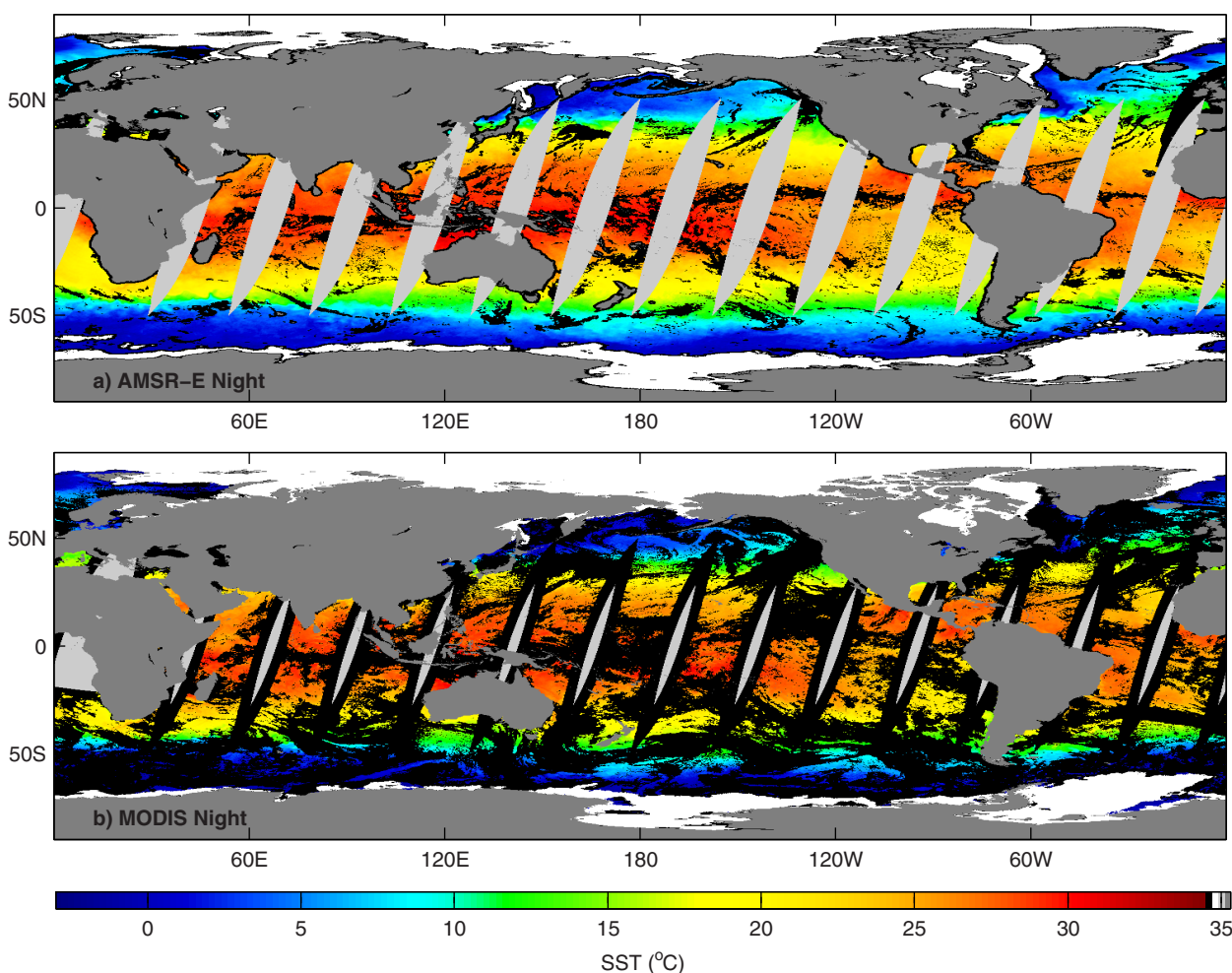
Figure 1. (a) AMSR-E and (b) MODIS night SSTs on 1 January 2003. Light gray areas are where no data are collected between successive orbits (swath gaps). Black areas show missing data. AMSR-E missing data are primarily due to rain, but additional missing data are visible near land and in the Northern Atlantic and Mediterranean due to RFI. MODIS shows narrower swath gaps then AMSR-E, but data at high incidence angles are of lower quality and therefore result in missing data at the scan edges. Most other missing data are due to the presence of cloud.

daily (Figure 1). Any errors in retrieved wind speed, water vapor, and cloud liquid water may result in errors in the retrieved SST. The AMSR-E SST spatial resolution is dictated by the 6.9 GHz channel footprint size, 74 km × 43 km, but is oversampled and gridded onto a 25 km grid. In Figure 1, there are the typical gaps between successive orbits at latitudes less than 45°. Missing data due to rain is seen as gaps within the swaths of data. In the upper right corner of the figure, near Ireland, there is a large gap that is due to RFI from a geostationary satellite.

There have been several studies published demonstrating the quality of previous versions of the AMSR-E SSTs. AMSR-E SST v4 retrievals were previously validated by *Dong et al.* [2006] against in situ expendable bathythermograph and hull-mounted thermosalinograph (TSG) data collected in the Southern Ocean on a research vessel. AMSR-E SSTs were found to have a bias of 0.24 K (summer) and −0.24 K (winter) when compared to the TSG data. These biases were attributed to errors in the geophysical retrieval algorithm for AMSR-E SSTs and were dependent on wind speed and atmospheric water vapor values.

O'Carroll et al. [2008] compared collocated buoy and satellite SSTs from both the Advanced Along-Track Scanning Radiometer (AATSR) and AMSR-E (v5). They reported a STD error of 0.42 K for AMSR-E SSTs.

Lean and Saunders [2013] compared AMSR-E v5 SST data from 2003 to 2009 to Along-Track Scanning Radiometer (ATSR) Reprocessing for Climate (ARC) and drifting buoy data. Collocation data were required to

have all three data sources provide valid SSTs within 3 h and 25 km of the in situ SST location. Using the three-way collocation analysis, they found AMSR-E errors for each year to be between 0.46 and 0.50 K. From 2003 to 2006, the error was 0.46 K, increasing to 0.50 K by 2009. In the paper, this was attributed to instrument degradation with age, but we believe it is more likely due to the increase in unflagged RFI contamination present in the later years. Since the onboard calibration of AMSR-E minimizes instrument performance degradation with age, increases in uncertainty are far more likely to be due to changes in the distribution of environmental parameters that contribute to retrieval errors or to a change in the accuracy of contaminated retrieval exclusion. For MW SSTs, excluding RFI contaminated retrievals is a difficult, constantly changing endeavor due to the sources of RFI: geostationary satellite TV broadcasts and ground-based communication systems. The satellite broadcasts are constantly changing and adapting to reach new subscribers or improve access for existing subscribers, while the ground-based communication systems can be extremely variable in their broadcast durations, frequency, and distribution.

Castro et al. [2012] compared drifting buoys to AMSR-E v5 SSTs from 2005 to 2008. Using only data within 25 km and 1 h of buoy location and time, they found a daytime bias and STD of 0.03 and 0.62 K and a nighttime bias and STD of 0.02 and 0.63 K. The day (night) collocations had 801,515 (970,311) pairs with 1875 (1871) unique buoys.

In this study, we use version-7 (v7) AMSR-E data. This updated geophysical retrieval algorithm has been improved and we expect to find lower error values for AMSR-E. No AMSR-E v6 existed as the numbering scheme for the MW geophysical retrieval algorithm was merged with that from SSM/I. The well-developed and validated SSM/I processing approach were unified with all other MW radiometers processed at Remote Sensing Systems (REMSS) resulting in the v7 designation.

2.2. MODIS

MODIS is also on the NASA Aqua satellite. The instrument has 36 spectral bands from 0.4 to 14.4 μm, measured $\pm55°$ from nadir, yielding a swath width of 2330 km, and a surface observation spatial resolution of 1 km at nadir. The SST algorithms use the 3.95, 4.05, 11, and 12 μm channels [*Minnett et al.*, 2004]. The MODIS 11–12 μm SST collection 5 is used in this study because it provides both day and night SST retrievals. Five minutes granules of MODIS data are processed by the NASA Goddard Ocean Biology Processing Group (OBPG using algorithms developed by the U. Miami Rosenstiel School for Marine and Atmospheric Science (RSMAS)) group. The MODIS observations have a nadir resolution of 1 km, but for this analysis we have averaged all best quality observations to 25 km for comparison with the 25 km gridded AMSR-E data.

The MODIS 11 μm SST algorithm [*Franz*, 2006] uses the nonlinear SST (NLSST) algorithm [*Walton*, 1988]. Algorithm coefficients are derived via collocations to in situ observations and are slowly varying, time dependent coefficients, of weighted means over a 3 month interval. The coefficients are additionally dependent on the difference between the 11 and 12 μm channels, with separate set of coefficients for when the difference is less than or equal to 0.5, between 0.5 and 0.9, and greater than or equal to 0.9. During the day, the first guess temperature is the short-wave algorithm SST, while at night the weekly Reynolds OISST product [*Reynolds et al.*, 2002] is bilinearly interpolated to the pixel location [*Brown and Minnett*, 1999].

Cloud screening is essential to the accuracy of IR SST products. The MODIS cloud identification algorithm is based on a decision tree of physically reasonable, spatial homogeneity, and differences-from-climatology tests. Errors in the MODIS SST data are primarily due to water vapor, trace gas, aerosol (from either or both volcanic and terrigenous sources) absorption, or undetected cloud [*Brown and Minnett*, 1999].

MODIS SST retrievals are assigned a quality level from 0 to 4, with 0 indicating the highest quality. High zenith angle, difference from a reference SST, presence of sun glint, cloud, or land, or values outside of range will all result in a quality level greater than 0. For this analysis, only quality 0 pixels are included, so the edges of the measurement swath and all cloud are masked (Figure 1). The cloud screening results in a significant loss of data as compared to the MW retrievals.

A global calculation of MODIS SST uncertainty, derived through buoy and M-AERI comparisons, using data from July 2002 to mid-2007 was given in *Minnett* [2010]. Collocated observations were required to be within 30 min and 10 km of each other. The buoy comparisons yielded a day(night) bias of $-0.15(-0.22)°$C and STD of $0.55(0.48)°$C. Comparisons to M-AERI showed a day(night) bias of $0.04(-0.02)°$C and STD of

0.59(0.53)°C. The SSTs in the comparison were not corrected for the skin effect or filtered for diurnal warming. The buoy comparisons show a larger negative bias then the M-AERI comparisons which are to be expected from the skin effect and a larger negative nighttime bias and lower STD which is to be expected as diurnal warming will impact daytime collocations. The same relationship is true for the M-AERI comparisons which should have an equal measurement of the diurnal cycle.

The MODIS SST retrievals are considered measurements of the skin layer SST [*Minnett et al.*, 2004]. To better compare these retrievals with MW and in situ SSTs the skin effect is modeled and removed using the cool skin correction from *Donlon et al.* [2002]. Using M-AERI data from a number of cruises, in both the Pacific and Atlantic Oceans, the nighttime SST measured by the M-AERI and other ship-board radiometers was compared to a ship mounted thermosalinograph (TSG) measured temperature at 1–5 m (depending on cruise), as a function of wind speed to develop an empirical cool skin estimate that only depends on instantaneous wind speed, u:

$$T_{skin} = -0.14 - 0.30 e^{\frac{-u}{3.7}} \tag{1}$$

Using the collocated AMSR-E wind speed, we estimate the cool skin effect and subtract it from the MODIS SSTs to form a subskin MODIS SST estimate that is used in all further analysis and collocations.

2.3. In Situ

In situ measurements collected from the existing network of fixed buoys, drifting buoys, and ship measurements are available via the Global Telecommunication System (GTS). These data are collected and distributed in near real-time (NRT) from the US Global Ocean Data Assimilation Experiment (USGODAE) server in Monterey. The data set used is called "SFCOBS" and contains surface observations from ships, moored, and drifting buoys, and CMAN in situ surface temperatures. Daily files contain the number of observations followed by the observation date, time, latitude, longitude, SST, probability of a gross error (assumes normal probability density function for SST errors [*Cummings*, 2011]), call sign, and data type (fixed buoy, drifting buoy, ship, etc.) [*Cummings*, 2006]. This in situ SST data set was used "as-is" with no additional data flagging except as described in section 3.

Castro et al. [2012] evaluated the accuracy of different types of moored and drifting buoys when used for validation of satellite SSTs. Manufacturer was not an indicator of performance for drifting buoys. Tropical moored buoys were similarly consistent. Nontropical moored buoys showed biases dependent on location, and it was unclear if this was a result of buoy calibration accuracy or satellite SST biases. Coastal moored buoys showed consistently large STDs relative to the SST products, but this was attributed to real geophysical differences between a point measurement and a spatial average in a highly spatially varying coastal regions.

3. Methodology

For this study, we use the AMSR-E 25 km grid and average the higher resolution MODIS SSTs to a 25 km grid for our collocation analysis. These grids are then used to identify matched buoys that are located within a given 25 km grid cell with valid data for both instruments. Ascending passes are considered daytime and descending passes are considered nighttime in this study.

At latitudes greater than 60°, the daily maps are virtually continuous as one swath begins to overlap with the other (Figure 1). Data were quality checked and prepared as described in the previous section. In the overlap regions, data are only averaged from a single swath to best preserve the satellite measurement time. In situ observations, which are organized into daily files, were collocated with satellite data from the previous, current, and following day, to ensure accurate collocation at the beginning and end of the daily in situ files. Figure 2 shows the STD of the satellite minus in situ SST plotted as a function of the in situ SST observation probability of gross error, a value calculated by FNMOC and distributed in the in situ data set (described in http://www.usgodae.org/ftp/outgoing/fnmoc/data/ocn/docs/ocn_obs.f). As shown, the estimate of error is effectively estimating error: as the probability of error increases, so does satellite minus in situ estimate STD. Based on these results, our analysis only uses in situ SST with a probability of gross error less than 0.6°C.
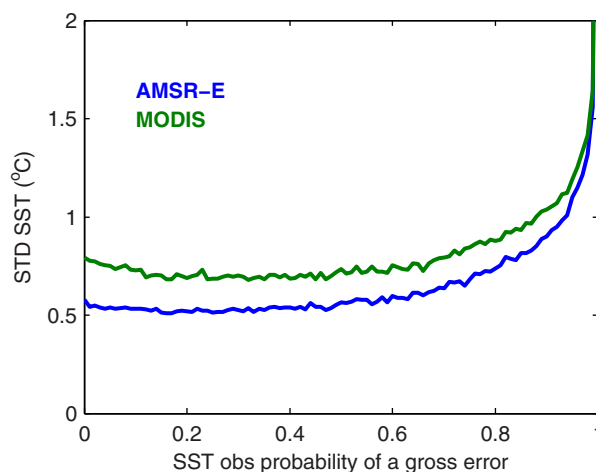
Figure 2. GTS buoy SST observation probability of a gross error as a function of the STD of both AMSR-E (blue) and MODIS (green) compared to buoy SSTs, including both day and night collocations. As the probability of error increases above 0.6, the STD rapidly increases.

Diurnal warming is a real geophysical process that will result in differences between the satellite and in situ measurements of SST. To improve our estimation of retrieval error it is necessary to exclude collocations that may have diurnal warming present. Figure 3 shows the day and night bias for both AMSR-E and MODIS minus the in situ data. The AMSR-E day and night biases are close in value and are centered on 0°C for winds above 6 m s^{-1}. Below 6 m s^{-1}, the night bias stays close to 0°C, while the day bias increases with decreasing wind speed, reaching a maximum of over 2.5°C at 0 m s^{-1}. This is a classic response and has been previously shown to be due to diurnal warming [*Gentemann and Wentz*, 2001]. The MODIS comparisons show a similar diurnal response as AMSR-E, but for both the day and night collocations there is a negative bias for winds greater than 6 m s^{-1}, with the night bias more negative than the day bias. This negative MODIS biasing will be investigated later in the paper. To avoid collocations with diurnal warming, all collocations between 10 A.M. and 4 P.M. (local time) with wind speeds less than 6 m s^{-1} are excluded from all further analyses.

Finally, we considered temporal collocation criteria. Figure 4 shows the bias (left column) and STD (right column) for daytime AMSR-E and MODIS collocations as a function of the satellite to in situ measurement time difference. Figures 4a and 4b show collocations with only the gross probability of error criteria applied to exclude bad collocations. (QC) and collocations with both QC applied and diurnal warming excluded (QC+DW). Both the bias and STDs increase with increasing collocation time differences. In Figure 4a, the bias variability is reduced when QC+DW is applied. In Figure 4b, the STD is reduced for both AMSR-E and MODIS collocations when both QC+DW are applied. These results demonstrate that excluding the diurnal events during the day is the correct methodology for estimating the true measurement error. Examining Figure 4b, the STD increases slowly up to a collocation measurement differe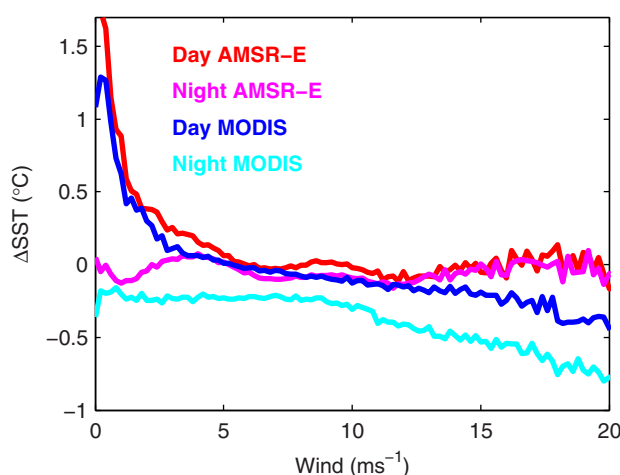nce of 3 h, after which it rises more rapidly. Although the STD is least with a collocation less than 1 h, this reduces the number of collocations from 417,368 to 35,322. Based on these results, we chose to exclude data affected by diurnal warming events (daytime observations 10 A.M. to 4 P.M. with wind speeds <6m s^{-1}) and measurement time differences greater than 3 h.

We also considered the measurement source in collocating data. Table 1 shows the uncertainties for AMSR-E and MODIS versus in situ comparisons by in situ data type. Both the AMSR-E and MODIS errors are largest for ship (intake, bucket, and hull sensor) type measurements, while the buoys (fixed, moored, and CMAN) have the lowest STDs. Drifting buoys have the largest number of
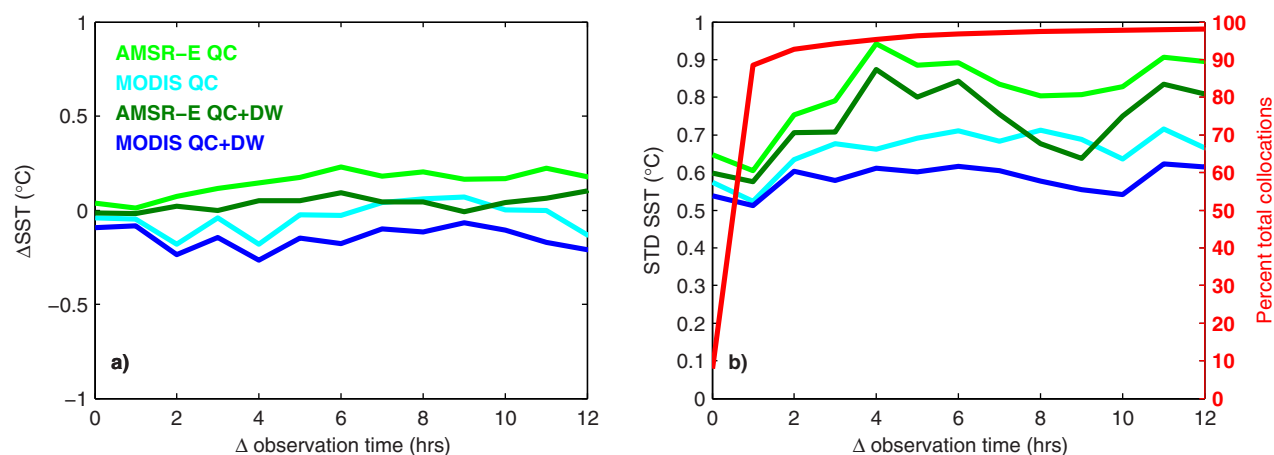

Figure 3. Mean biases (satellite minus buoy) shown as a function of wind speed for day and night observations. AMSR-E day and night biases are indistinguishable from each other above 10 m s^{-1} wind speed. Below 6 m s^{-1} the day bias diverges rapidly from the night bias, with the bias increasing as wind speed decreases. This is clear evidence of the diurnal warming effect on the satellite measurements.

Figure 4. Temporal collocation errors, with the bias as a function of the difference in observation time (a) between the collocated buoy and satellite observation and (b) the standard deviation. The light green (AMSR-E) and turquoise (MODIS) have only the probability of gross error quality control flag applied. The darker green (AMSR-E) and darker blue (MODIS) show the same quantities, but with the additional diurnal warming quality control applied. Figure 4b also shows the percent of total collocations included for each temporal window.

collocations, likely due to the significant number of buoys and their greater spatial coverage. Based on the results in this table, we chose to use only the fixed and drifting buoys, and CMAN stations in our analysis. Ship data are frequently used in analyses despite the largest STDs [*Kaplan et al.*, 1998; *Rayner et al.*, 2006] due to their long record.

4. Global Errors

Based on the methodology described above, the comparisons in this study included only those values for which we had all three collocations within a 3 h collocation time window, using only buoy (fixed, drifting, and CMAN) values with a gross probability of error of less than 0.6, and having applied a diurnal warming criteria to mask possible diurnal warming events. Histograms of the AMSR-E and MODIS day/night differences as a function of SST are shown in Figure 5. The night MODIS comparisons show large differences at low SSTs. The global distribution of satellite minus buoy biases is shown in Figure 6. The top row shows day biases for both the AMSR-E and MODIS comparisons, while the middle row shows night biases. The left column shows AMSR-E results, while the right column shows results for MODIS. The collocations are fairly uniformly distributed (Figure 7), with a high number of collocations at the tropical moored buoy locations and more nighttime collocations due to removing daytime diurnal warming affected data. Figures 6e and 6f show the new nighttime collocations, there are less north of 50°N and few south of 50°S.

O'Carroll et al. [2008] found negative biases at 45°N and positive biases at 45°S when comparing AMSR-E v4 to buoy SSTs. These biases may have been remnant errors in the calibration technique or RFI contaminated retrievals that were not excluded in the AMSR-E v4 data. The v7 AMSR-E data used in this comparison do not show any biasing similar to that shown in the O'Carroll results.

Table 1. Individual In Situ Data Type Uncertainties for Triple Collocations[a]

	AMSR-E—In Situ		MODIS—In Situ		
	Bias (°C)	STD (°C)	Bias (°C)	STD (°C)	Number
Engine intake	−0.02	0.74	−0.29	0.85	12,910
Fixed buoy	−0.02	0.55	−0.27	0.69	33,474
Drifting buoy	−0.04	0.50	−0.19	0.67	370,972
Bucket	0.00	0.73	−0.17	0.84	1260
Hull sensor	−0.06	0.69	−0.31	0.81	4912
CMAN	0.08	0.56	−0.23	0.54	103

[a]Collocations were excluded if the in situ data had a gross probability of error >0.6 or the measurement time difference exceeded 3 h. A cool skin correction was applied to the MODIS data. Over 9 years, the number of collocations per day equals roughly 10 for fixed and 113 for drifting buoys. This table shows the analysis of errors for the distributed data sets without any corrections applied.
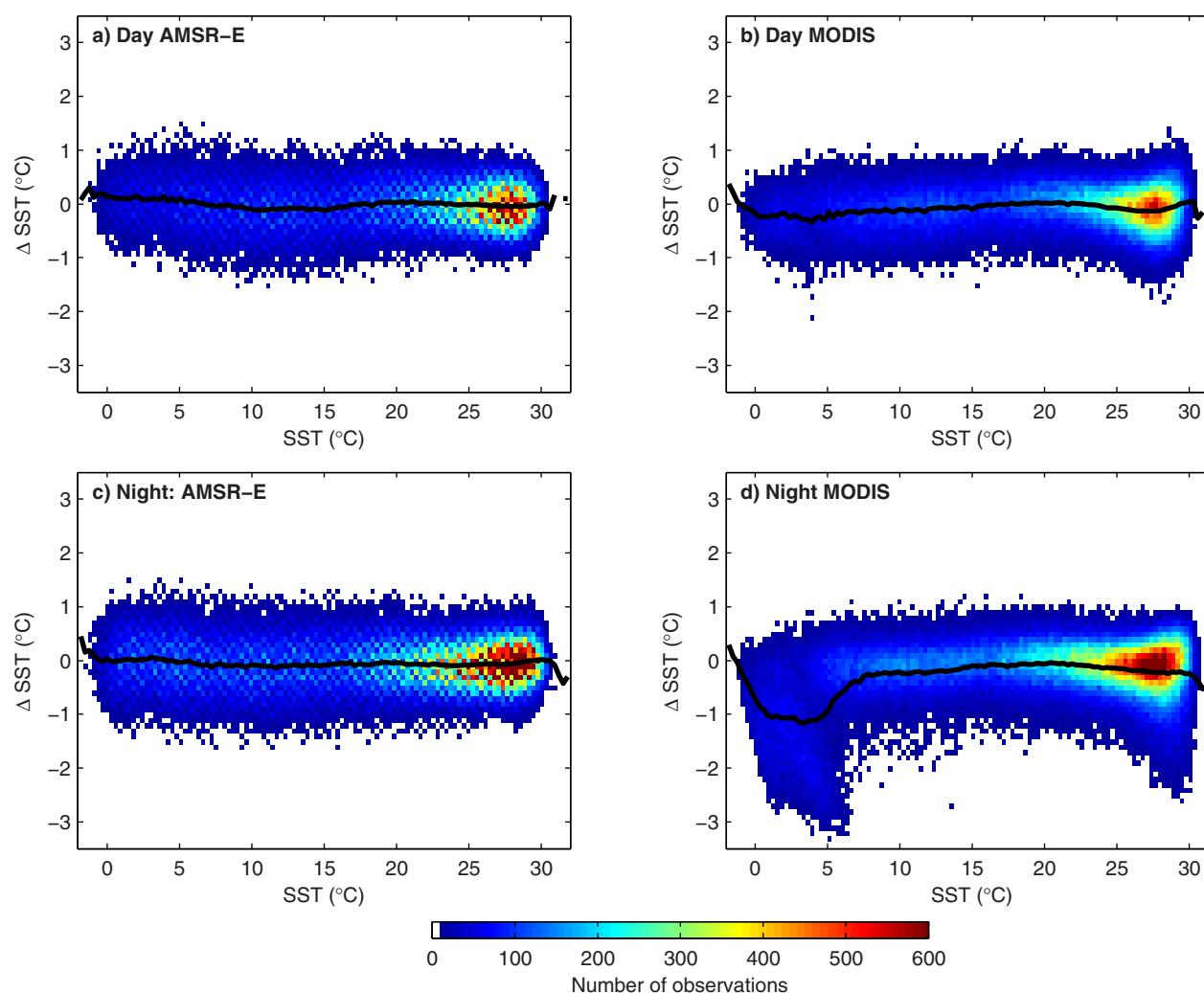
Figure 5. PDF of biases for (a) AMSR-E day, (b) MODIS day, (c) AMSR-E night, and (d) MODIS night. The mean bias is shown by a solid black line in each plot. MODIS night SSTs in Figure 5d have large negative biases at low SSTs.

Figure 6d shows the MODIS night global biases. There are large cold biases in the Southern Hemisphere at high latitudes that are not present in the day (Figure 6b). These biases appear to follow and exist below the Antarctic circumpolar front. We examined daily MODIS and AMSR-E SST images to determine the source of this strong regional bias and found large biases near cloud masked regions suggesting that the issue might be cloud screening in the nighttime MODIS SST retrievals. To further examine this, the biases for AMSR-E and MODIS minus buoy data were examined as a function of SST and AMSR-E cloud liquid water (Figure 8). The day (top row) and night (bottom row) mean biases for AMSR-E minus buoy and MODIS minus buoy are shown as a function of cloud liquid water (x axis) and SST (color of line). The values of cloud liquid water are all very low; normal distribution is from 0 to 2.5 mm, while here valid data have values between 0 and 0.15 mm. This is because the triple collocations are only made in clear skies. The triple collocation requires a clear sky for the IR SST retrieval and heavy cloud is likely identified and masked. Because the IR SST is from a 1 km retrieval that is then remapped to a 25 km grid, it is possible that measurements of AMSR-E low cloud liquid water 25km grid cells may very well contain IR values from partially cloudy skies where MODIS has both accurate and valid retrievals in clear sky and masked retrievals in cloudy skies. The 25 km clear sky SST retrievals match to a low cloud amount from the lower resolution microwave retrieval. The daytime comparisons for both MODIS and AMSR-E and night AMSR-E all show good results with little dependence on cloud. The night MODIS comparisons show a distinct and large dependence on cloud liquid water at SST values
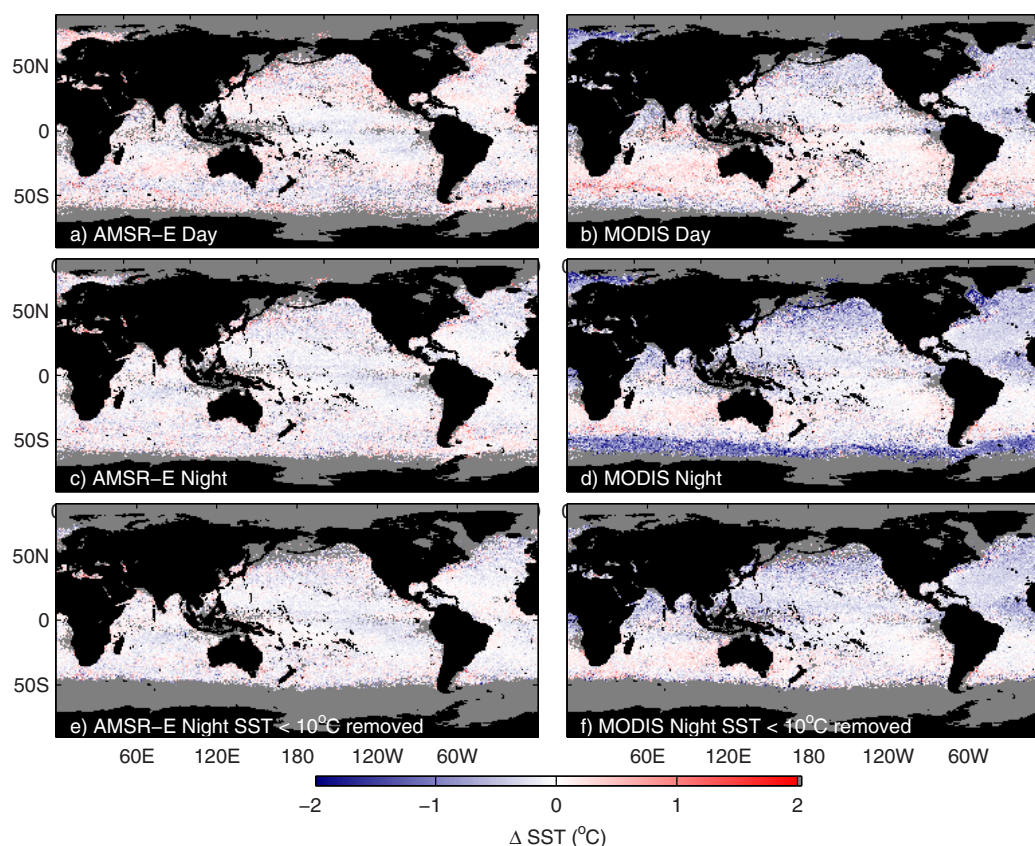
Figure 6. Global distribution of the mean biases, satellite minus buoy SSTs, 4 July 2002–4 October 2011. While AMSR-E shows little structure or coherent features in the mean bias, MODIS shows a distinct cool bias in cooler waters in both the Northern hemisphere and a small warm bias in the Southern Hemisphere. (a and b) AMSR-E and MODIS day biases. (c and d) Night biases. (e and f) The global biases with the additional check that removes night collocations where SST is less than 10°C. Because the collocation requires all three SSTs, with the additional check, Figures 6e and 6f both show almost no collocations below ∼50°S and a significant reduction in collocations above 50°N.
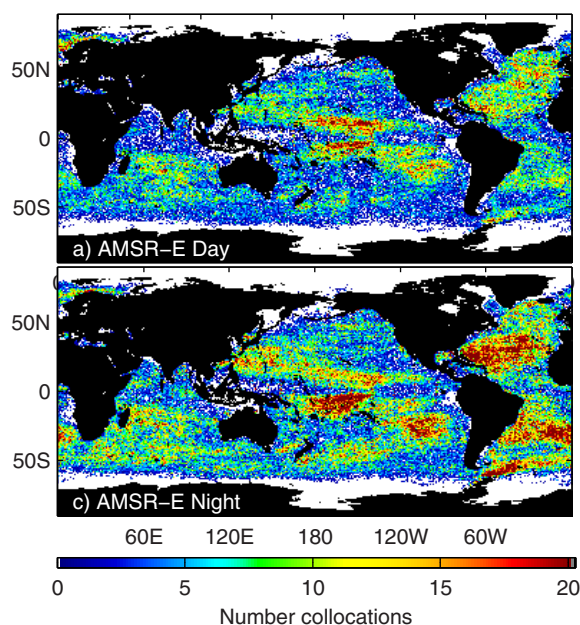

Figure 7. Number of collocations for day and night. The satellite-buoy collocations are a triple collocation, so the number of collocations is the same for the AMSR-E and MODIS data in Figure 6.

less than 10°C. The biases increase with increasing cloud amounts. This result indicates that nighttime MODIS SST retrievals over cold water are not sufficiently well screen for cloud. For this reason, we exclude in our results the nighttime MODIS retrievals that have SSTs less than 10°C. Global biasing was again checked and this mask removed much of the large high latitude negative biases, as seen in Figure 6f.

A small cool bias remains in MODIS in the central eastern Atlantic Ocean (Figures 6b and 6f). This is a region long associated with the presence of aerosols that are known to affect IR SSTs [*Chan and Gao*, 2005; *Nalli and Stowe*, 2002]. There also appears to be some North-South biasing, with small warm biases in the Southern hemisphere and a cool bias in the Northern hemisphere. AMSR-E shows relatively minimal biasing (Figures 6a and a). The day is slightly noisier than the night biases.
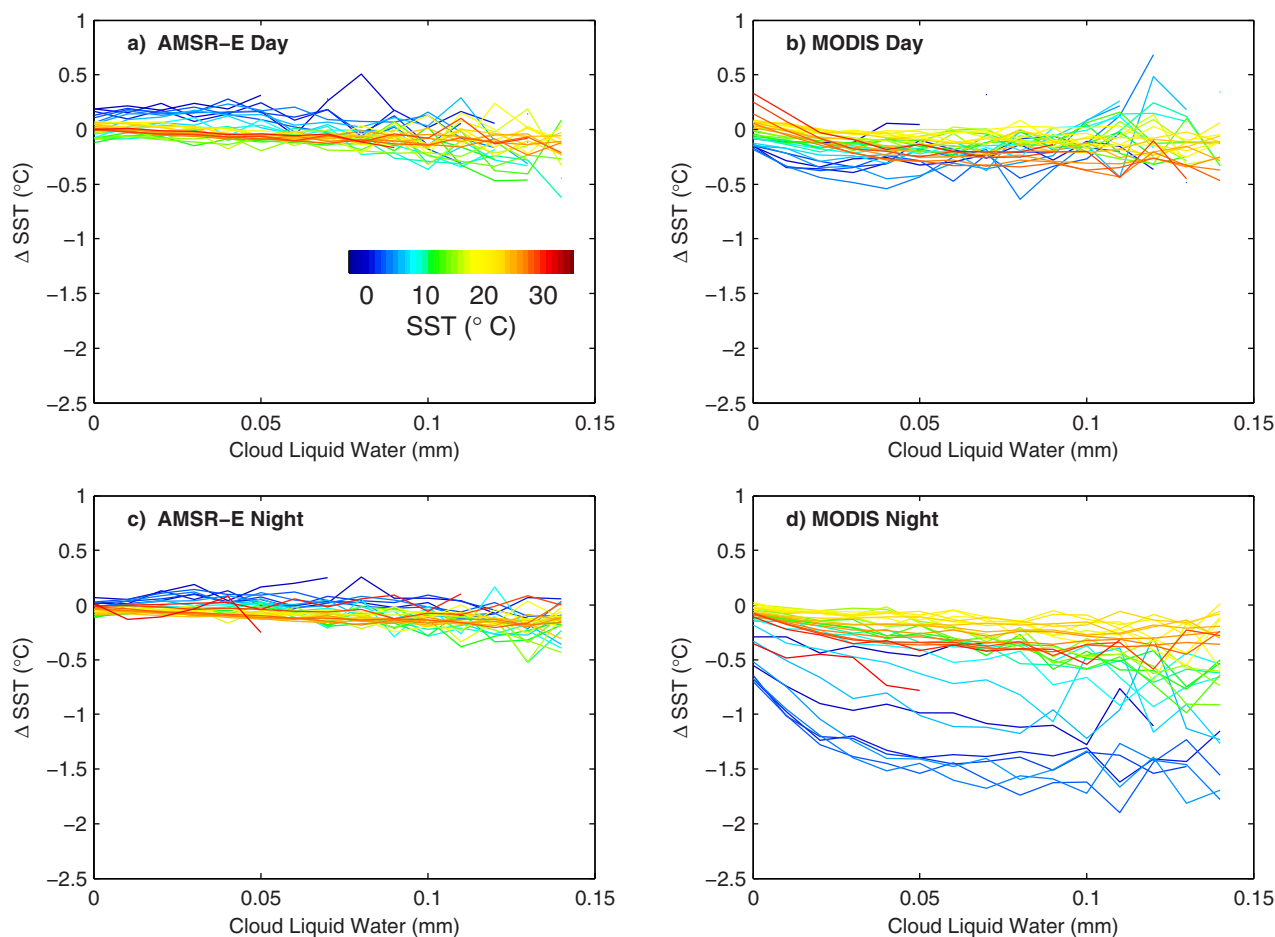
Figure 8. Satellite minus buoy SST as a function of cloud liquid water (*x* axis) and SST (color of lines). (a and c) AMSR-E day and night observations have no dependence on SST or cloud. (b) A slight warm bias at very low cloud water amounts, for only the warmest of day MODIS SSTs. (d) At nighttime, MODIS SSTs have bias dependent on cloud amount at cold SSTs.

There is a slight cool bias in the Tropical Pacific and a slight warm bias in the day high Southern hemisphere.

Figure 9 shows the AMSR-E and MODIS uncertainties as a function of SST and water vapor, which are highly correlated [*Stephens*, 1990]. AMSR-E shows a small warm bias at SSTs <10°C, while MODIS shows a slight cool bias in the same temperature range. The same relationship is seen for water vapor less than 10 mm, with AMSR-E bias becoming increasingly positive and MODIS bias increasingly negative for decreasing water vapor values. It is difficult to ascribe this characteristic to either SST product, since it could be one or both of them. The distribution of data for these low SST and vapor values are shown in Figure 9 (right). To ensure that the region in the Northeast Atlantic that is often contaminated with RFI is not dominating the AMSR-E results, the analysis was rerun, but with the RFI region excluded. The same results were found, so we confidently feel the observed biases are not an artifact of RFI. We next separated the Northern and Southern Hemispheres to test the results. Similar results were found for both hemispheres. The dependencies on SST <10°C and vapor <10 mm was robust in both hemispheres for both AMSR-E and MODIS retrievals.

Based on the low vapor bias results, we examined the AMSR-E v7 processing software and found a small software coding error. A posthoc SST correction used to reduce an SST dependence on water vapor was not applied correctly. The vapor dependence correction was removed from the AMSR-E SSTs and the data were reexamined. By randomly selecting half of the collocations, a new correction was developed and then tested on the independent half of the data. To correct the coding error, the following correction should be applied to the data:
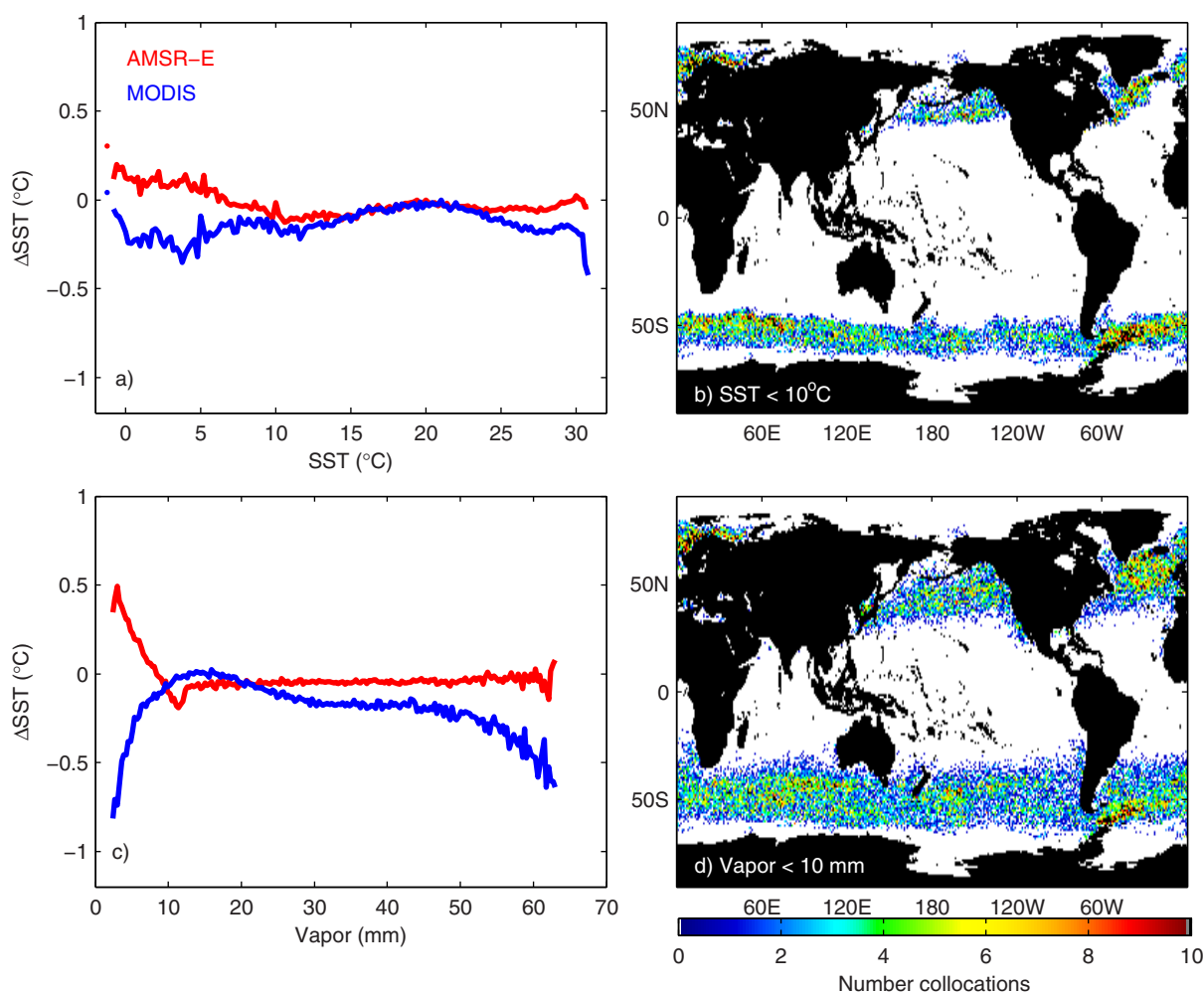
Figure 9. Satellite SST minus buoy SST as a function of (a) SST and (c) vapor. There is no dependence on SST for either AMSR-E or MODIS above 8°C. Night collocations for SST less than 10°C were excluded prior to this result due to cloud contamination. (a) A warm bias in AMSR-E and a cold bias in MODIS at SST below 8°C. (c) AMSR-E has is no dependence on water vapor until vapor less than 10 mm where AMSR-E has a warm bias and that MODIS has a cool bias below about 10 mm and above 45 mm. The distribution of collocations for (b) SST less than 8°C is shown and (d) vapor less than 10 mm.

$$\text{SST}_{v7a} = \text{SST}_{v7} + \frac{0.7}{64}(8 - \text{vapor})^2; \quad \text{when } 10 \text{ mm} <= \text{vapor} < 12 \text{ mm} \qquad (2)$$

$$\text{SST}_{v7a} = \text{SST}_{v7} + \frac{0.7}{64}(8 - \text{vapor})^2 - \frac{1.15}{10^{1.52}}(10 - \text{vapor})^{1.52}; \quad \text{when } \text{vapor} < 10 \text{ mm} \qquad (3)$$

SST_{v7a} is the corrected AMSR-E v7 SST (SST_{v7}), vapor is the AMSR-E v7 columnar water vapor (mm) which is distributed in the SST data product file available from Remote Sensing Systems. Equation (2) is used to calculate the correction when vapor is greater than or equal to 10 mm and less than 12 mm. Equation (3) is used when vapor is less than 10 mm. The randomly selected data not used in developing the correction were then used to test the correction in Figure 10. The STD are shown as dashed lines around the mean bias for AMSR-E v7 (before correction; red) and AMSR-E v7a (after correction; blue). The dependency on water vapor and SST is improved. It is recommended that all AMSR-E v7 users apply this correction prior to performing any analysis. The updated correction has only a small impact on the overall errors after the correction is applied as the low water vapor values exist infrequently and represent only 10.5% of the total collocations used in the study. Bias and STD by in situ data type and overall collocations, with the vapor correction are given in Tables 2 and 3. This error is also found in the REMSS WindSAT v7.0.1 SSTs and the correction given above should be applied.
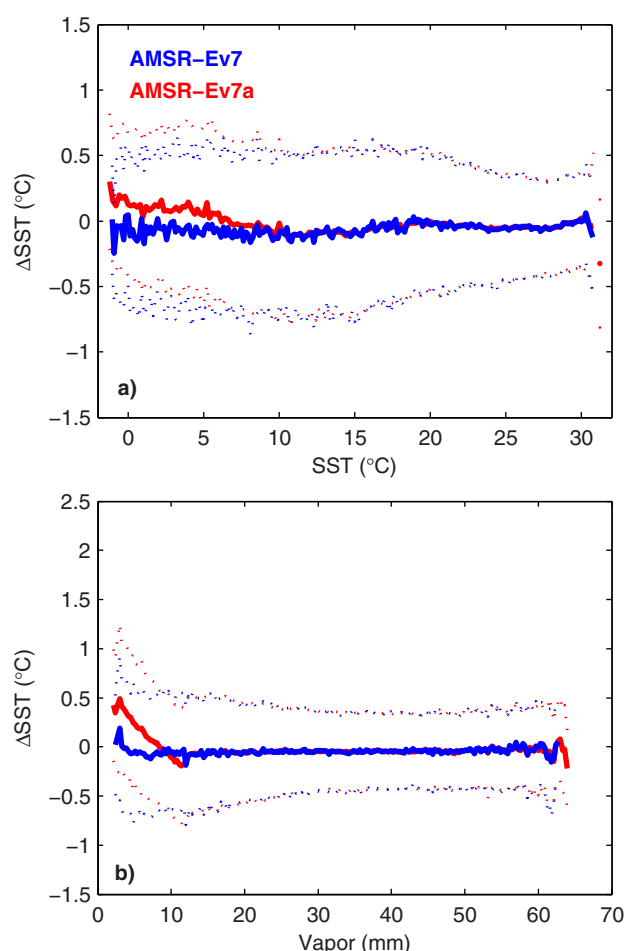
Figure 10. AMSR-E minus buoy as a function of (a) SST and (b) vapor for AMSR-E v7 (red) and AMSR-E v7a (with correction; blue). The correction removes both the SST and vapor dependency seen in AMSR-E v7 data.

The onboard calibration for both MODIS and AMSR-E should minimize long-term drifts in the SST data, but erroneous trends can still manifest if sources of errors change over time. For example, RFI significantly increased in location and extent during the operational lifetime of AMSR-E [*Gentemann et al.*, 2010b]. Since RFI flagging and removal is a difficult and constantly changing exercise, it is plausible that new sources are not adequately removed over time, leading to increased biases and errors in the AMSR-E data. Additionally, changing terrigenous or volcanic aerosols can manifest as trends in the MODIS data if not adequately screened.

To demonstrate how uncertainty may change with time, Figure 11 shows a Hovmöller plot of the average monthly SST uncertainties for the zonally averaged 1° latitude bins. The latitudinal distribution of the collocations is clearly changing over the period from 2002 to 2011 due to the changing locations of the drifting buoys. Figure 11e shows the number of collocations, in which one can see the increase in buoy measurement of high-latitude regions over time and a sharp increase in more tropical collocations after 2004. The AMSR-E biases (Figure 11a) are fairly consistent with latitude from 2002 to mid-2007 when the drifting buoys start to be deployed at or drift to higher latitudes. These higher latitudes show a slight warm bias. The AMSR-E STD (Figure 11c) is lowest from 40°S to 40°N, and increases with increasing latitude. There is a slight seasonal cycle to the STD. Figure 11b shows the MODIS biases which are lowest in the Southern Hemisphere. There is a small negative bias in the Northern Hemisphere that increases with latitude. The MODIS STD (Figure 11d) is fairly consistent for all latitudes, but does show some seasonal fluctuations in peak values.

The biases and higher STDs in the AMSR-E SSTs are likely not due to RFI which is mostly located in the Northern Hemisphere whereas the errors are high in both the Northern and Southern higher latitudes. The

Table 2. Individual In Situ Data Type Uncertainties for All Triple Collocations Except Those Excluded for Diurnal Contamination or MODIS Night Retrievals Less Than 10°C[a]

	AMSR-E—In Situ		MODIS—In Situ		
	Bias (°C)	STD (°C)	Bias (°C)	STD (°C)	
Ship engine intake	−0.01	0.72	−0.22	0.78	11,386
Fixed buoy	−0.03	0.53	−0.21	0.63	30,412
Drifting buoy	−0.05	0.48	−0.12	0.57	325,115
Ship bucket	0.05	0.70	−0.10	0.80	1101
Ship hull sensor	−0.06	0.69	−0.27	0.76	4429
CMAN	0.09	0.55	−0.20	0.55	95

[a]These results are with the AMSR-E SST correction applied (equations (2) and (3)).

Table 3. Uncertainties for Triple Collocation With Drifting, Fixed, and CMAN Buoy Measurements[a]

	Ascending (Day)			Descending (Night)			All		
	Bias (°C)	STD	Number	Bias (°C)	STD	Number	Bias (°C)	STD	Number
AMSR-E—buoy	−0.04	0.50	83,149	−0.07	0.47	95,204	−0.05	0.48	178,353
MODIS—buoy	−0.09	0.58	83,149	−0.16	0.58	95,204	−0.13	0.58	178,353
AMSR-E—MODIS	0.05	0.67	83,149	0.09	0.65	95,204	0.07	0.66	178,353

[a]Collocations were excluded if the buoy data had a gross probability of error >0.6, the measurement time difference exceeded 3 h, daytime wind speed less than 6 m/s (diurnal contamination), or night SST was less than 10°C. A cool skin correction was applied to the MODIS data. These results use only the independent random half of the data that was not used to develop the vapor correction.

MW algorithm requires wind direction for SST retrieval and in these regions of fast moving storms and fronts, wind direction error may be larger and result in increased uncertainty.

Figure 12 shows a 30 day running mean of all three collocated SSTs (Figure 12a), biases (Figure 12b), and STDs (Figure 12c) for AMSR-E and MODIS compared to buoys. Figure 11 shows the change in polar coverage, so the bias and STD were determined only using collocations between 40°S and 40°N. The mean bias
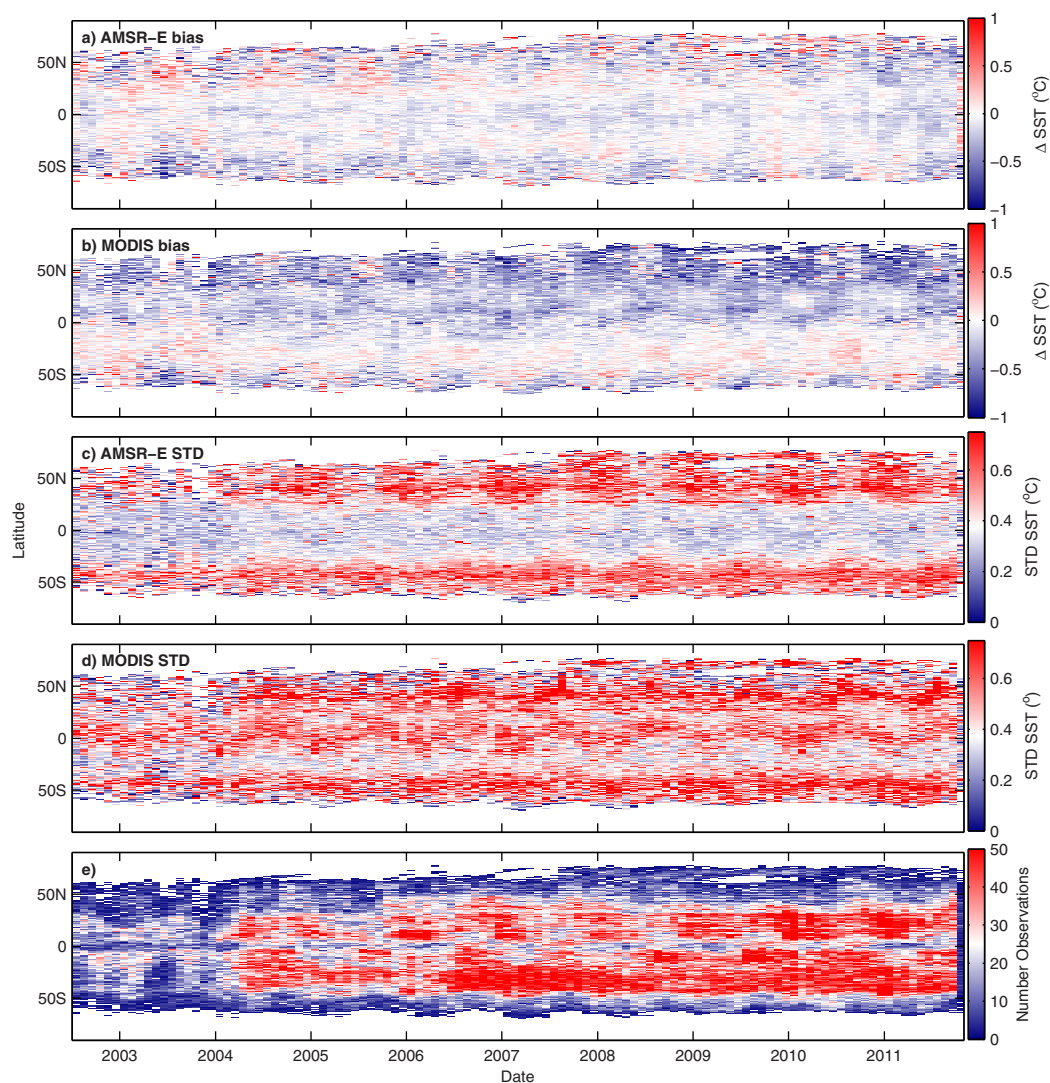

Figure 11. Hovmoller plot for month averages of the bias and standard deviation shown by Latitude and Date. From top to bottom (a) AMSR-E—buoy bias, (b) MODIS—buoy bias, (c) AMSR-E minus buoy standard deviation, (d) MODIS minus buoy standard deviation, and (e) number of collocations.
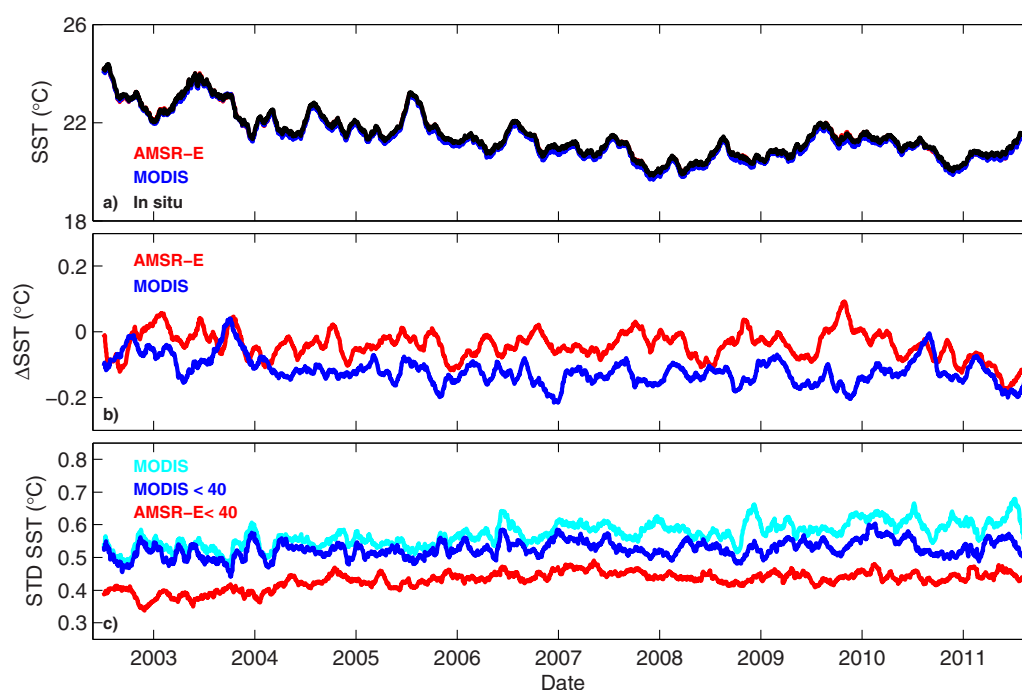
Figure 12. Time series of SST, biases, and STD, 4 July 2002–4 October 2011, where the data were smoothed with a running 30 day running mean. (a) The average SSTs for AMSR-E, MODIS, and buoy, (b) the mean biases, and (c) the STD. Figure 12c shows that the MODIS standard deviation increases almost 0.1°C from 2003 to 2011 when using global collocations. Restricting the calculation to data from 40°S to 40°N removes the increasing trend in the uncertainty which is a sampling artifact.

is mostly stable and variability similar for both comparisons for entire record. There is no pronounced seasonal cycle to the bias. After 2010, AMSR-E appears to have a slight increasing negative trend in the bias which brings the bias toward agreement with the MODIS bias. The MODIS bias is stable for the entire record with a small negative bias. The STD (Figure 12c) is shown for the latitudinally restricted collocations and for all collocations from MODIS (in cyan). In Figure 12c, using all collocations, the MODIS STD (turquoise line) shows a slow, constant increase in error. This is related to the increase in sampling of the higher latitudes, as shown in Figure 11. The blue and red lines show the MODIS and AMSR-E STDs, using only data 40°S–40°N. When using the regions that are equally sampled, the STD remains constant in time, indicating that both instruments are performing well through 2011.

Table 4. Triple Collocation Derived Individual Buoy Data Standard Deviations

	STD (°C)
Ship engine room intake	0.37
Fixed buoy	0.24
Drifting buoy	0.20
Ship bucket	0.34
Ship hull sensor	0.36
CMAN	0.25

Table 5. Triple Collocation Derived Individual Satellite and Buoy Standard Deviations

	STD (°C)
AMSR-E	0.28
MODIS	0.38
Buoy	0.20

5. Three-Way Error Analysis

Uncertainties for day, night, and all collocations are shown in Table 3. All questionable data have been removed as detailed above. The day and night STDs are similar for each collocation pair, indicating that the diurnal and additional cloud exclusions are working sufficiently well.

A three-way error analysis was developed for validation of wind speeds by *Stoffelen* [1998] and used for SST validation by *Blackmore et al.* [2007] and *O'Carroll et al.* [2008]. The STD for each observation type is determined using collocations of the three different data types. For more details, a derivation and discussion is included in the appendix of *O'Carroll et al.* [2008]. The analysis assumes that errors are uncorrelated. *O'Carroll et al.* [2008] tested this assumption for IR, MW, and in situ collocated SSTs and found it to be valid. The observation error variance for the three observation types is

$$\sigma_1{}^2 = \frac{1}{2}\left(V_{12} + V_{31} - V_{23}\right)$$

$$\sigma_2{}^2 = \frac{1}{2}\left(V_{23} + V_{12} - V_{31}\right) \qquad (4)$$

$$\sigma_3{}^2 = \frac{1}{2}\left(V_{31} + V_{23} - V_{12}\right)$$

where 1, 2, and 3 indicate the observation types and V_{12} is the variance of the difference between observation types 1 and 2. Observation errors were determined in two different manners. First, the individual errors for each buoy measurement type were determined and are shown in Table 4, using triple collocations restricted to each buoy measurement type. Table 4 shows that drifting buoys have the lowest error, followed with increasing errors by fixed buoys, CMAN stations, ship bucket thermometers, ship hull sensors, and ship engine room intake temperatures. This result may be partially explained by the fact that a component of this derived error is due to spatial variability at the location of the triple collocation, and drifting buoys are most often in the open ocean where local spatial variability is small. Many fixed buoys are in the open ocean, but a significant number are in coastal regions with higher spatial variability. Since all different types of in situ observations are used for climate SST analyses, an estimate of their error by this method is of interest.

Next, using all the buoy collocations, Table 5 shows errors by observation type are 0.20°C for buoy, 0.28°C for AMSR-E, and 0.38°C for MODIS. The larger MODIS errors are partly explained by aerosol or cloud contamination. As expected, the buoy measurements have the least error. In this analysis, the MW AMSR-E SSTs have less error then the IR MODIS SSTs. This global database using AMSR-E v7 data from 2002 to 2011 shows far less error than derived by other investigators using previous versions of AMSR-E SST data [*Castro et al.*, 2012; *Dong et al.*, 2006; *O'Carroll et al.*, 2008].

6. Conclusions

A global analysis of the distribution of satellite minus buoy biases revealed problems in both AMSR-E and MODIS SST products. Solutions have been suggested to correct for a water vapor dependency in AMSR-E and to minimize nighttime cloud contamination in MODIS. It is recommended that all AMSR-E v7 users apply the AMSR-E vapor correction determined in this paper prior to performing any analysis. Even after these corrections there remain two issues with MODIS SSTs. (1) There remains a cold bias in MODIS at high latitudes that is a dependence on water vapor and/or SST. (2) There is a North-South hemisphere biasing (warm in South and cold in North) that is not easily explained. After the correction, AMSR-E shows minimal regional biases, with the night biases and STD less than daytime biases and STD.

The AQUA satellite is ideal for a triple collocation validation study as it has collocated independent MW and IR SST measurements from the AMSR-E and MODIS instruments. Using data from 2003, and AMSR-E v5 data, *O'Carroll et al.* [2008] found STDs of 0.14°C for AATSR, 0.24°C for buoy, and 0.42°C for AMSR-E v5 SSTs. Our results show AMSR-E v7 data have improved significantly, with a STD of 0.28°C. Buoy errors were similar at 0.20°C, just slightly less than the 0.24°C found by O'Carroll. MODIS errors were found to be 0.38°C. The larger STD in the MODIS retrievals is an unexpected result. Table 3 shows both day and night MODIS retrievals have a STD of 0.58°C. This is about 0.1°C higher than results given by *Minnett et al.* [2004] and could be attributed to possible errors in cloud removal, aerosol contaminated retrievals, or sampling (due to the 25 km averages and/or different regions).

A Hovmöller plot and a time series of mean biases and STD revealed the importance of sampling. A simple time series of bias and STD shows false trends in bias and STD that are related to sampling. Once sampling is accounted for by restricting the latitudinal range of collocation pairs used in the time series analysis, the trend was eliminated and both instruments appear to be stable.

The IPCC Working Group I contribution to the IPCC fifth assessment report final draft [*Hartmann et al.*, 2013] and *Reynolds et al.* [2010] state that MW SSTs are less accurate but provide better coverage then IR SSTs. This is mostly based on error analysis of high-resolution IR SSTs to buoy data sets and comparing results to separate analyses of the lower resolution MW SSTs compared to buoy data sets. Here we find that the MW AMSR-E SSTs have less error then the IR MODIS SSTs. It is likely that the MODIS SST uncertainty would be reduced with better removal of cloud contaminated data. Additionally, there is a contribution to the MODIS SST uncertainty

from sampling error caused by clouds present in the 25 km average used for this analysis. As both data sets evolve, generalized statements like this are unlikely to be an accurate assessment of retrieval skill.

References

Blackmore, T., A. G. O'Carroll, R. W. Saunders, and H. H. Aumann (2007), Numerical weather prediction: A comparison of sea surface temperature from the AATSR and AIRS instruments, *Forecasting Res. Tech. Rep. 499*, 21 pp., Met Off., Exeter, U. K.

Brown, O. B., and P. J. Minnett (1999), *MODIS Infrared Sea Surface Temperature Algorithm*, p. 98, Univ. of Miami, Miami, Fla.

Castro, S. L., G. A. Wick, and W. J. Emery (2012), Evaluation of the relative performance of sea surface temperature measurements from different types of drifting and moored buoys using satellite-derived reference products, *J. Geophys. Res.*, 117, C02029, doi:10.1029/2011JC007472.

Chan, P.-K., and B.-C. Gao (2005), A comparison of MODIS, NCEP, and TMI sea surface temperature datasets, *IEEE Geosci. Remote Sens. Lett.*, 2(3), 270–274, doi:10.1109/LGRS.2005.846838.

Cummings, J. (2006), The NRL real-time ocean data quality control system, NRL Tech. Note.

Cummings, J. (2011), Ocean data quality control, in *Operational Oceanography in the 21st Century*, edited by A. Schiller and G. B. Brassington, pp. 91–121, Springer, Netherlands, doi:10.1007/978-94-007-0332-2_4.

Dong, S., S. T. Gille, J. Sprintall, and C. L. Gentemann (2006), Validation of the Advanced Microwave Scanning Radiometer for the Earth Observing System (AMSR-E) sea surface temperature in the Southern Ocean, *J. Geophys. Res.*, 111, C04002, doi:10.1029/2005JC002934.

Donlon, C. J., P. J. Minnett, C. L. Gentemann, T. J. Nightingale, I. J. Barton, B. Ward, and M. J. Murray (2002), Toward improved validation of satellite sea surface skin temperature measurements for climate research, *J. Clim.*, 15(4), 353–369.

Franz, B. (2006), *Implementation of SST Processing Within the OBPG*, NASA Ocean Biol. Process. Group.

Gentemann, C. L., and F. J. Wentz (2001), Satellite microwave SST: Accuracy, comparisons to AVHRR and Reynolds SST, and measurement of diurnal thermocline variability, in *Proceedings of the IEEE International Geoscience and Remote Sensing Symposium, IGARSS'01*, pp. 246–248, Sydney, Australia, doi: 10.1109/IGARSS.2001.976116.

Gentemann, C. L., T. Meissner, and F. J. Wentz (2010a), Accuracy of satellite sea surface temperatures at 7 and 11 GHz, *IEEE Trans. Geosci. Remote Sens.*, 48(3), 1009–1018.

Gentemann, C. L., F. J. Wentz, M. Brewer, K. A. Hilburn, and D. K. Smith (2010b), Passive microwave remote sensing of the ocean: An overview, in *Oceanography from Space, Revisited*, edited by V. Barale et al., pp. 13–33, Springer, Heidelberg, Germany.

Hartmann, D. L., A. Klein Tank, and M. Rusticucci (2013), Working Group I Contribution to the IPCC Fifth Assessment Report (AR5) Climate Change 2013: The physical science basis, final draft, 2216 pp., Intergov. Panel on Clim. Change, Stockholm.

Jessup, A. T., and R. Branch (2008), Integrated ocean skin and bulk temperature measurements using the Calibrated InfraRed *In Situ* Measurement System (CIRIMS) and through-hull ports, *J. Atmos. Oceanic Technol.*, 25, 579–597.

Kaplan, A., M. A. Cane, Y. Kushnir, A. C. Clement, M. Benno Blumenthal, and B. Rajagopalan (1998), Analyses of global sea surface temperature 1856–1991, *J. Geophys. Res.*, 103(C9), 18,567–18,589, doi:10.1029/97JC01736.

Lean, K., and R. W. Saunders (2013), Validation of the ATSR Reprocessing for Climate (ARC) dataset using data from drifting buoys and a three-way error analysis, *J. Clim.*, 26(13), 4758–4772.

Lumpkin, R., and M. Pazos (2007), Measuring surface currents with surface velocity program drifters: The instrument, its data, and some recent results, in *Lagrangian Analysis and Prediction of Coastal and Ocean Dynamics*, edited by A. Griffa et al., pp. 39–67, Cambridge Univ. Press, Cambridge, U. K.

Minnett, P. J. (2010), The validation of sea surface temperature retrievals from spaceborne infrared radiometers, in *Oceanography From Space, Revisited*, edited by V. Barale et al., pp. 273–295, Springer, Heidelberg, Germany.

Minnett, P. J., O. B. Brown, R. E. Evans, E. L. Key, E. J. Kearns, K. A. Kilpatrick, A. Kumar, K. A. Maillet, and M. Szczodrak (2004), Sea-surface temperature measurements from the Moderate-Resolution Imaging Spectroradiometer (MODIS) on Aqua and Terra, in *Proceedings of the IEEE International Geoscience and Remote Sensing Symposium, IGARSS '04*, 7, 4576–4579, Anchorage, Alaska, doi:10.1109/IGARSS.2004.1370173.

Minnett, P. J., M. Smith, and B. Ward (2011), Measurements of the oceanic thermal skin effect, *Deep Sea Res., Part II*, 58(6), 861–868, doi:10.1016/j.dsr2.2010.10.024.

Nalli, N. R., and L. Stowe (2002), Aerosol correction for remotely sensed sea surface temperatures from the national oceanic and atmospheric administration advanced very high resolution radiometer, *J. Geophys. Res.*, 107(C10), 3172, doi:10.1029/2001JC001162.

O'Carroll, A. G., J. R. Eyre, and R. W. Saunders (2008) Three-way error analysis between AATSR, AMSR-E, and in situ sea surface temperature observations, *J. Atmos. Oceanic Technol.*, 25, 1197–1207.

Price, J. F., R. A. Weller, and R. Pinkel (1986), Diurnal cycling: Observations and models of the upper ocean response to diurnal heating, cooling, and wind mixing, *J. Geophys. Res.*, 91(C7), 8411–8427.

Rayner, N. A., P. Brohan, D. E. Parker, C. K. Folland, J. J. Kennedy, M. Vanicek, T. J. Ansell, and S. F. B. Tett (2006), Improved analyses of changes and uncertainties in sea surface temperature measured *in situ* since the mid-Nineteenth century: The HadSST2 dataset, *J. Clim.*, 19(3), 446–469.

Reynolds, R. W., N. A. Rayner, T. M. Smith, D. C. Stokes, and W. Wang (2002), An improved *in situ* and satellite SST analysis for climate, *J. Clim.*, 15, 1609–1625.

Reynolds, R. W., C. L. Gentemann, and G. K. Corlett (2010), Evaluation of AATSR and TMI Satellite SST data, *J. Clim.*, 23(1), 152–165.

Soloviev, A., and R. B. Lukas (1997), Observations of large diurnal warming events in the near-surface layer of the western equatorial Pacific warm pool, *Deep Sea Res., Part I*, 44(6), 1055–1076.

Stephens, G. L. (1990), On the relationship between water vapor over the oceans and sea surface temperature, *J. Clim.*, 3(6), 634–645.

Stoffelen, A. (1998), Toward the true near-surface wind speed: Error modeling and calibration using triple collocation, *J. Geophys. Res.*, 103(C4), 7755–7766.

Walton, C. C. (1988), Nonlinear multichannel algorithms for estimating sea surface temperature with AVHRR satellite data, *J. Appl. Meteorol.*, 27, 115–124.

Ward, B. (2006), Near-surface ocean temperature, *J. Geophys. Res.*, 111, C02005, doi:10.1029/2004JC002689.

Webster, P. J., C. A. Clayson, and J. A. Curry (1996), Clouds, radiation, and the diurnal cycle of sea surface temperature in the tropical western Pacific, *J. Clim.*, 9, 1712–1730.

Wentz, F. J., and T. Meissner (2000), *AMSR Ocean Algorithm, Version 2*, vol. 121599A-1, p. 66, Remote Sens. Syst., Santa Rosa, Calif.

Wentz, F. J., C. L. Gentemann, D. K. Smith, and D. B. Chelton (2000), Satellite measurements of sea surface temperature through clouds, *Science*, 288(5467), 847–850.